HHS Public Access

Author manuscript

Cancer Res. Author manuscript; available in PMC 2017 March 01.

Published in final edited form as:

Cancer Res. 2016 March 1; 76(5): 1055–1065. doi:10.1158/0008-5472.CAN-14-3630.

An immune-inflammation gene expression signature in prostate tumors of smokers

Robyn L. Prueitt[#1], **Tiffany A. Wallace**[#1], **Sharon A. Glynn**[#1,*], **Ming Yi**[2], **Wei Tang**[1], **Jun Luo**[3], **Tiffany H. Dorsey**[1], **Katherine E. Stagliano**[4], **John W. Gillespie**[5], **Robert S. Hudson**[1], **Atsushi Terunuma**[1], **Jennifer L. Shoe**[6], **Diana C. Haines**[7], **Harris G. Yfantis**[8], **Misop Han**[3], **Damali N. Martin**[1], **Symone V. Jordan**[1], **James F. Borin**[9], **Michael J. Naslund**[9], **Richard B. Alexander**[9], **Robert M. Stephens**[2], **Christopher A. Loffredo**[10], **Dong H. Lee**[8], **Nagireddy Putluri**[11], **Arun Sreekumar**[11], **Arthur A. Hurwitz**[5], and **Stefan Ambs**[1]

[1]Laboratory of Human Carcinogenesis, Center for Cancer Research (CCR), National Cancer Institute (NCI), National Institutes of Health (NIH), Bethesda, MD, USA

[2]Advanced Biomedical Computing Center, Leidos Biomedical Research/NCI, Frederick, MD, USA

[3]Department of Urology, Johns Hopkins Medical Institutions, Baltimore, MD, USA

[4]Laboratory of Molecular Immunoregulation, CCR, NCI, NIH, Frederick, MD, USA

[5]Laboratory of Pathology and Urologic Oncology Branch, CCR, NCI, NIH, Bethesda, MD, USA

[6]Laboratory Animal Sciences Program, Leidos Biomedical Research, Frederick National Laboratory, Frederick, MD, USA

[7]Pathology/Histotechnology Laboratory, Leidos Biomedical Research, Frederick National Laboratory, Frederick, MD, USA

[8]Pathology and Laboratory Medicine, Baltimore Veterans Affairs Medical Center, Baltimore, MD, USA

[9]Urology and Greenebaum Cancer Center, University of Maryland, MD, USA

[10]Cancer Prevention and Control Program, Lombardi Comprehensive Cancer Center, Georgetown University Medical Center, Washington, DC, USA

[11]Department of Molecular and Cell Biology, Verna and Marrs McLean Department of Biochemistry, Alkek Center for Molecular Discovery, Baylor College of Medicine, Houston, TX 77030, USA

[#] These authors contributed equally to this work.

Abstract

Smokers develop metastatic prostate cancer more frequently than nonsmokers, suggesting that a tobacco-derived factor is driving metastatic progression. To identify smoking-induced alterations

Correspondence to: Stefan Ambs, Laboratory of Human Carcinogenesis, National Cancer Institute, Bldg.37/Room 3050B, Bethesda, MD 20892-4258. Phone 301-496-4668; ambss@mail.nih.gov.

[*]Current Adress Sharon Glynn Lambe Institute/Translational Research Facility School of Medicine, NUI Galway Galway, Ireland

Conflicts of interest: We declare that no conflicts of interest exit.

in human prostate cancer, we analyzed gene and protein expression patterns in tumors collected from current, past, and never smokers. By this route, we elucidated a distinct pattern of molecular alterations characterized by an immune and inflammation signature in tumors from current smokers that were either attenuated or absent in past and never smokers. Specifically, this signature included elevated immunoglobulin expression by tumor-infiltrating B cells, NF-κB activation, and increased chemokine expression. In an alternate approach to characterize smoking-induced oncogenic alterations, we also explored the effects of nicotine in human prostate cancer cells and prostate cancer-prone TRAMP mice. These investigations showed that nicotine increased glutamine consumption and invasiveness of cancer cells *in vitro* and accelerated metastatic progression in tumor-bearing TRAMP mice. Overall, our findings suggested that nicotine was sufficient to induce a phenotype resembling the epidemiology of smoking-associated prostate cancer progression, illuminating a novel candidate driver underlying metastatic prostate cancer in current smokers.

Keywords

Prostate cancer; tobacco smoking; gene expression profiles; nicotine

INTRODUCTION

Prostate cancer is a leading cause of cancer mortality among men (1). Few environmental factors have been consistently associated with prostate cancer (2). While cigarette smoking may not influence early disease development (3, 4), it increases the risk of fatal prostate cancer (3, 5, 6). This observation was replicated in studies showing that current smokers develop distant metastasis more frequently than nonsmokers (7, 8). Because smoking cessation reduces the risk of metastasis (3, 6), a tobacco-related factor appears to induce reversible molecular alterations in prostate cancer that facilitate metastatic spread.

Here, we pursued a two-fold hypothesis. First, we explored whether prostate tumors from current smokers have a gene expression profile that differentiates them from tumors of never or past smokers. Secondly, because nicotine can activate oncogenic signaling pathways that promote cancer progression (9, 10), we also explored its effects in human prostate cancer cell lines and prostate cancer-prone TRAMP mice to evaluate whether they resemble the epidemiology of smoking-associated prostate cancer progression. Using these approaches, we identified a distinct immune and inflammation signature in prostate tumors of current smokers. We also found that physiologic concentrations of nicotine induce Akt pathway activation and metabolic changes, and increase invasiveness of human prostate cancer cells. Lastly, nicotine accelerated the onset of metastasis in TRAMP mice.

MATERIALS & METHODS

Tissue collection and cell lines

Sixty-seven fresh-frozen prostate tumors were obtained from the NCI Cooperative Prostate Cancer Tissue Resource (CPCTR) (n = 37), Department of Pathology, University of Maryland (UMD; n = 10), and Department of Urology, Johns Hopkins Medical Institutions

(JHU; n = 20). Additional 69 formalin-fixed, paraffin-embedded (FFPE) tumor specimens were collected at UMD. Tissue collection was approved by the institutional review boards at the participating institutions. Written informed consent was obtained from all donors. CPCTR has been described (11). Smoking information at time of surgery (current, past, never) was obtained from medical records and cancer registry entries for CPCTR and JHU. For patients from UMD, this information was abstracted from an epidemiological questionnaire. The human immortalized prostate epithelial cell line, RWPE-1, and human prostate cancer cell lines (22Rv1, PC-3, LNCaP, DU145) were obtained from the American Type Culture Collection (Manassas, VA) between 2006 to 2010. Authentication of these cell lines was performed in December, 2013, using a short tandem repeat analysis with GenePrint10 (9 loci + amelogenin for sex determination). For details on tissue collection and assessment of smoking status see Supplementary Methods.

RNA extraction from frozen bulk tissue and cell lines

Tissue macrodissection and isolation of total RNA from tissues and cell lines was performed according to standard methods described in Supplementary Methods.

Affymetrix microarrays

RNA labeling and hybridization were performed according to Affymetrix standard protocols (Santa Clara, CA), as described (12). Labeled cRNA was hybridized either to Affymetrix GeneChip HG-U133A 2.0 or mouse 1.0 ST arrays. In accordance with Minimum Information About a Microarray Experiment (MIAME) guidelines, we deposited the CEL files for the microarray data and additional patient information into the GEO repository (http://www.ncbi.nlm.nih.gov/geo/). The GEO submission accession number for the 47 bulk tissue tumors, which were initially analyzed, is GSE6956. GSE68138 contains the gene expression data for the additional 20 bulk tissue tumors (“JHU samples”) and the laser capture microdissected tumor samples (n=10), and for prostate tumors from TRAMP mice +/− nicotine treatment (n=10), and cell lines (22Rv1 and LNCaP cells) +/− nicotine treatment (n=12). For more information, see Supplementary Methods.

RNA isolation from microdissected prostate tumors

Enriched tumor epithelium was obtained from 5 current and 5 never smokers with laser capture microdissection (LCM) of frozen tissue samples. These tumors were also analyzed as bulk tissues. 5,000 to 15,000 cells per tumor were collected. RNA was isolated using the PicoPure protocol (Arcturus, Mountain View, CA). mRNA was amplified with two linear amplification steps by *in vitro* transcription using the MEGAscript T7 kit (Ambion, Austin, TX) followed by labeling using the BioArray HighYield RNA Transcript Labeling Kit T3 from Enzo Life Sciences (Farmingdale, NY). Labeled cRNA was hybridized onto arrays.

Data normalization and statistical analysis of gene expression data

All chips were normalized using the RMA procedure (13). Because two sets of array data were analyzed for human prostate tumors, we controlled for a batch effect using the Partek Genomics Suite (www.partek.com) or the Bioconductor limma R package (www.bioconductor.org). To generate lists of differently expressed genes, the resulting data

sets were subjected to the significance analysis of microarray procedure (14) or linear modeling features implemented in limma. Supplementary Tables S7-11 describe differentially expressed genes in LCM tumor epithelium comparing current (n = 5) versus never smokers (n = 5) (S7-S8), nicotine-treated (n = 3) vs. untreated (n = 3) 22Rv1 and LNCaP cells (S9-S10), and prostate tumors from nicotine-treated (n = 5) vs. untreated (n = 5) TRAMP mice (S11), respectively. For more information, see Supplementary Methods.

GSEA analysis

Gene Set Enrichment Analysis (GSEA) was performed as described (15). For details see Supplementary Methods.

Quantitative Real-time PCR of gene expression

See Supplementary Methods.

In situ hybridization for immunoglobulin kappa and lambda light chain expression in prostate tumors and immunohistochemistry

See Supplementary Methods.

Proliferation, motility, and invasion assays of nicotine-treated cells

See Supplementary Methods.

Integrin cell surface expression and extracellular matrix (ECM) protein binding assays

See Supplementary Methods.

Western blot analysis of nicotine-treated cells

See Supplementary Methods.

Measurement of IL-8 in human plasma samples

See Supplementary Methods.

Glutamine consumption in nicotine-treated prostate cancer cells

22Rv1 and LNCaP cells were plated in T150 flasks, serum starved, and treated with 100 nM nicotine. One ml of media was collected and cell pellets were prepared. Dried extracts of these samples were re-suspended in injection solvent composed of water:methanol (50:50) and subjected to Liquid Chromatography/Mass Spectrometry. Details can be found in Supplementary Methods.

Nicotine treatment of prostate cancer-prone TRAMP mice and evaluation of lung metastasis

Male TRAMP mice were bred at the Assisted Reproduction Laboratory, Frederick National Laboratory for Cancer Research, Frederick, Maryland, using *in vitro* fertilization (B6xFVB F1). At 8 to 9 weeks of age they received either tap water or a solution of either 100 or 250 μg/ml of nicotine in tap water, which is similar to a previous described protocol (16). The three groups consisted of 20-25 animals each. At the selected concentration, nicotine

generates nicotine plasma concentrations comparable to those of active smokers and causes some weight loss (Supplementary Figure S1). All mice were euthanized after 80 days or when they became moribund because of prostate cancer. To assess the effects of nicotine on prostate cancer development and metastasis, the prostate glands and lungs were collected and were formalin-fixed for histological examination by a boarded veterinary pathologist. All described animal procedures were reviewed and approved by the NCI-Frederick Institutional Biosafety Committee (IBC registration #06-060 and 11-041). NCI-Frederick is accredited by AAALAC International and follows the Public Health Service Policy for the Care and Use of Laboratory Animals. More details can be found in Supplementary Methods.

Statistical analysis

Statistical analyses were performed using STATA (Stata Corp, College Station, TX) or GraphPad Prism 6 (GraphPad Software, La Jolla, CA). All statistical tests were two-sided and an association was considered statistically significant with $P < 0.05$. The Spearman rank correlation (e.g., for continuous B cell numbers in never, past, current smokers) or the Fisher's exact tests (e.g., for nuclear p-NF-κB stratified into present or absent in never, past, current smokers) were used to calculate P_{trend}. The Wilcoxon rank-sum test was used as a non-parametric statistical test to compare two independent groups. Comparisons among more than two independent groups were performed with the ANOVA and Kruskal-Wallace tests.

RESULTS

A smoking-associated gene expression signature in prostate tumors

We evaluated gene expression characteristics from tumors comparing current with past and never smokers. Patients are described in Supplementary Table S1: current, past and never smokers did not differ significantly by age, race/ethnicity, or clinicopathology. Initially, we analyzed the gene expression profiles of 47 tumors from 9 current, 21 past, and 17 never smokers using Affymetrix GeneChip microarrays. This analysis revealed an immune signature in tumors from current smokers. The most upregulated transcripts among current smokers represented immunoglobulins (Supplementary Table S2). When we performed a hierarchical cluster analysis, immunoglobulin expression separated tumors into two clusters (Figure 1). Tumors from current smokers were significantly over-represented in cluster 2, which consisted of tumors with up-regulated immunoglobulin expression. Furthermore, we applied a linear regression model to examine whether the differences in immunoglobulin expression by smoking status are confounded by race/ethnicity and found that these differences were independent of race/ethnicity.

To further investigate the immunoglobulin signature, we conducted *in-situ* hybridization (ISH) for signature validation, and to localize expression. ISH for both kappa and lambda light chain mRNA expression was performed on additional 22 FFPE tumors (6 current, 7 past, 9 never smokers). This approach revealed an elevated number of immunoglobulin-expressing B lymphocytes in tumors of current smokers compared with past and never smokers (Figure 2). The lymphocytes infiltrated the tumor stroma (Figure 2A & B and Supplementary Figure S2). Average number of lambda light chain-positive B lymphocytes

per 250x field increased from 3.6 (range: 0 to 24) among never smokers to 5 (range: 0 to 16) among past smokers to 23 (range: 1 to 86) among current smokers (Spearman rank correlation, $\rho = 0.51$; $P = 0.02$) (Figure 2C & D).

Because our initial analysis described only few genes other than immunoglobulins as being altered in tumors from current smokers, gene expression profiles from additional patients (JHU dataset: 7 current, 7 past, 6 never smokers) were combined with the discovery dataset to allow identification of more genes that are differently expressed between current and never/past smokers. For the combined dataset (67 tumors), we generated two gene lists using Significance Analysis of Microarrays: one for differently expressed genes between current (n = 16) and never smokers (n = 23), and one for differently expressed genes between current (n = 16) and never/past smokers (n = 51). The comparison of tumors from current and never smokers yielded 98 transcripts that represented 73 differentially expressed genes at a false-discovery rate ≤ 30% (Supplementary Table S3). The second comparison, current versus never/past smokers, yielded 70 transcripts representing 40 differently expressed genes (Supplementary Table S4). Notably, many of the differentially expressed genes in the two lists have known immune-regulatory functions, and their expression was increased in current smokers [e.g., immunoglobulins, indolamine-2,3-dioxygenase (*IDO1*) and chemokines]. Quantitative (q)RT-PCR analysis confirmed over-expression of immunoglobulins (*IGH*,*IGK*,*IGL*), *IDO1*, and several chemokines (*CCL5*, *CXCL10*, *CXCL11*) among current smokers in an analysis of 57 tumors (15 current, 18 never, 24 past smokers) from the microarray study (Supplementary Figure S3) while *CXCL8* (IL-8) did not validate. Expression of these immune genes tended to be low or absent in tumors from never or past smokers. Lastly, we generated additional gene lists for classification using Bioconductor limma R (Supplemental Figure S4). Differentially expressed genes were then assessed using the linear modeling features implemented in limma. *P* values < 0.05 were used to generate two gene lists for current vs. never and current vs. never/smokers. Probesets with same differential expression in both gene lists (n = 601, Supplementary Table S5) were selected for classification. As shown in Figure 3, the gene expression pattern defined by these probesets separated the 67 tumors into two clusters with greatly different gene expression. Up-regulation of genes in immune-related pathways was the main characteristic of tumors from current smokers that differentiated them from others.

Nuclear accumulation of NF-κB in tumors and increased IL-8 in blood of current smokers

Next, we tested whether increased stress signaling through NF-κB may occur in tumors from smokers because B cell activation has been linked to NF-κB signaling (17). We used immunohistochemistry (IHC) to determine nuclear localization of phosphorylated NF-κB, p65 subunit (Ser^{536}), in the tumor epithelium as described (18), to assess NF-κB activation (Figure 4A & B). Analyzing 69 tumors, we found nuclear NF-κB pSer536 in 5/26 tumors from never smokers (19%), 12/24 tumors from past smokers (50%), and 11/19 tumors from current smokers (58%) (P_{trend}=0.014; Fisher's exact test). Thus, accumulation of phosphorylated NF-κB correlated with smoking status. Because our microarray analysis initially indicated that IL-8 is up-regulated in tumors from current smokers, we also examined plasma levels of IL-8 in 97 prostate cancer patients and 89 controls to assess whether circulating IL-8 is increased in patients who are current smokers. The analysis

showed that IL-8 levels were significantly elevated in plasma from current smokers with prostate cancer (Figure 4C), but not among current smokers without the disease (Figure 4D).

Gene set enrichment analysis (GSEA)

We used GSEA to identify common features between the smoking-related gene signature in prostate tumors, nicotine-induced gene signatures in human prostate cancer cells, and archived signatures in the Molecular Signatures Database (MSIGDB) [http://www.broad.mit.edu/gsea/msigdb; (15)]. We aimed to identify candidate mechanisms by which smoking may induce gene expression alterations in the cancerous prostate, and to better define possible roles of nicotine.

Four signatures were subjected to GSEA. The first contained genes that were differentially expressed between current and never smokers in bulk tumors. The second signature was derived from the same contrast, but used microdissected tumor epithelium from 5 current and 5 never smokers as the source for the mRNA. The last two signatures were generated from LNCaP and 22Rv1 prostate cancer cells treated with 100 nM nicotine (vs. untreated), which is within the physiological concentration range for nicotine in current smokers (~10 to 500 nmol/l blood) (19, 20). Results are summarized in Supplementary Figure S5. In short, a hepatocyte growth factor (HGF)-induced gene signature in monocytes (21) and a glutamine starvation signature (22) were the two MSIGDB-archived gene signatures with significant associations among all four gene lists. The data suggest that nicotine may influence cell metabolism, leading to increased glutamine consumption, and also exerts functions that may mimic HGF in human prostate tumors. Glutamine deprivation can occur when glutamine is excessively metabolized, and it has been shown that glutamine deprivation leads to NF-κB activation (23). To validate this GSEA prediction, we examined glutamine consumption of nicotine-treated prostate cancer cells. As shown in Figure 5A & B, nicotine increased glutamine consumption in these cells, resulting in glutamine deprivation in culture medium.

Nicotine activates the Akt pathway and induces a pro-metastatic phenotype

Nicotine may have pro-metastatic properties in prostate cancer patients. We tested this hypothesis but first examined whether nicotinic acetylcholine receptors (nAChR) are expressed in the cancerous prostate. qRT-PCR showed that various nAChR subunits are expressed in prostate tumors and cancer cell lines (Supplementary Figure S6). Notably, the nAChR α7 subunit, which has been linked to PI3K-Akt pathway activation and other oncogenic effects (24), was significantly up-regulated in tumors. Next, we investigated whether nicotine activates oncogenic Akt signaling in human prostate cancer cell lines and in RWPE-1 immortalized prostate epithelial cells. Treatment of 22Rv1 prostate cancer cells with 10 nM and 100 nM nicotine led to phosphorylation of Akt (the key activating step for Akt) and its downstream targets, e.g., GSK3β and human MDM2 (Figure 5C-E). Akt pathway activation was also observed in other cell lines (Supplementary Figure S7). Both mecamylamine, an inhibitor of nAChR signaling, and the PI3 kinase inhibitor, LY294002, blocked nicotine-induced Akt phosphorylation (Figure 5D and Supplementary Figure S7B). Next, we assessed whether nicotine can induce a metastatic phenotype in prostate cancer cells and evaluated migration and matrigel invasion in response to nicotine. Nicotine enhanced matrigel invasion of both 22Rv1 and PC-3 cells (Figure 6A & B), which further

increased when nicotine and HGF were added together (Figure 6C). However, only nicotine-induced, but not HGF-induced, invasion was inhibited by mecamylamine (Figure 6D). Nicotine also enhanced migration of 22Rv1 cells but did not increase it in PC-3 cells (Supplementary Figure S8). Our findings suggest that nicotine may selectively enhance invasive properties of prostate cancer cells. This hypothesis was further supported by the observation that nicotine affected cell surface integrin expression and extracellular matrix binding, as nicotine increased binding of 22Rv1 cells to the bone-associated filaments, collagen type I and IV (Supplementary Figure S9), which is associated with metastasis-promoting integrin signaling (25, 26).

Nicotine accelerates the onset of metastasis in TRAMP mice

Our experiments showed that nicotine induces metastasis-related phenotypes in cell culture. For further corroboration, we evaluated the effect of nicotine on metastasis in TRAMP mice, which develop aggressive prostate tumors at 100% penetrance and start to develop visible pulmonary metastatic lesions at 24 weeks of age (27). We treated animals with 100 or 250 μg of nicotine/ml in the drinking water (n = 20-25) and assessed primary tumor growth and metastasis to the lung after 80 days of treatment. Our treatment regimens yielded an average 34 nM (5.5 ± 5.2 ng nicotine/ml, n = 6) or 105 nM (17.1 ± 9.0 ng/ml, n = 6) plasma nicotine concentrations, respectively, while nicotine was undetectable in untreated animals ($P < 0.01$). Nicotine did not increase the size of the cancerous prostate (Table 1), consistent with our observation that 100 nM nicotine either did not or only modestly enhance proliferation of RWPE-1, 22Rv1 or PC-3 cells (Supplementary Figure S10 & S11). In addition, we did not observe significant histological differences in the cancerous prostate between the treatment groups. However, the nicotine treatment produced metastatic lesions in the lung that were not present in control animals (Table 1), indicating it accelerates the onset of metastasis in this model. A total of 13 out of 45 nicotine-treated animals (29%) were positive for lung metastasis, compared to none of the 20 controls ($P = 0.006$, Fisher's exact test). To gain insights on the nicotine-induced molecular alterations, we analyzed gene expression in the cancerous prostate of untreated and 250 μg/ml nicotine-treated TRAMP mice (n = 5 each group). The analysis showed that nicotine-treated tumors have increased expression of genes regulating synaptic signal transduction (Supplementary Table S6). An Ingenuity pathway analysis also suggested an association of the differentially expressed genes with G2/M DNA damage checkpoint regulation ($P = 1.1\times10^{-6}$), mitotic roles of Polo-like kinases ($P = 6.6\times10^{-6}$), and the complement system ($P = 4.7\times10^{-5}$), and their strongest disease association was with cancer ($P = 3.4\times10^{-13}$). Lastly, we did not observe an immune signature with B cell infiltration in these tumors.

DISCUSSION

In this study, we describe an immune and inflammation signature in prostate tumors from current smokers. We further discovered that nicotine increases invasiveness of human prostate cancer cells and accelerates the onset of metastases in tumor-bearing TRAMP mice. These observations point to previously unrecognized mechanisms by which smoking may enhance prostate cancer progression. While mechanistically novel, they are in agreement with epidemiological studies and a recent publication describing inflammation in prostate

tumors of current smokers (28). Also, a systematic review of the relationship between smokeless tobacco and cancer revealed that prostate cancer is one of few cancers associated with the use of smokeless tobacco (29), which is a key source of nicotine and nicotine-derived nitrosamines, which both activate nAChRs (9, 10, 30).

Our analysis of prostate tumors indicated an increased presence of immunoglobulin-expressing B cells in tumors of current smokers while nicotine did not increase their numbers in tumors of TRAMP mice. B cell numbers are commonly increased in human prostate tumors, but this increase was not found to correlate with standard markers of disease aggressiveness (31). While their presence in primary tumors may not immediately have a progression-enhancing effect, their increase in current smokers could be deleterious at the transition to a castration-resistant disease (CRPC). It was shown that B cells accelerate this transition in a CRPC mouse model while B-cell depletion delayed CRPC development (32). The critical role of tumor infiltrating B cells was attributed to lymphotoxin-β secretion enhancing inflammation in the animal study. We examined lymphotoxin-β plasma levels in prostate cancer patients but could not detect elevated lymphotoxin-β in current smokers (Supplemental Figure S12). Perhaps, increased lymphotoxin-β is restricted to the tumor microenvironment. Alternatively, B cells may require stimuli for lymphotoxin-β release that specifically arise in the environment of CRPC.

Several studies reported that B cells enhance cancer development. In a mouse model of skin carcinogenesis, cancer progression driven by chronic inflammation was shown to be B cell-dependent (33). Here, deposition of circulating immune complexes into the tumor parenchyma led to the release of pro-angiogenic and pro-metastatic molecules (34). Similarly, we observed NF-κB activation and increased expression of chemokines in prostate tumors of current smokers with high B cell counts, indicative of a pro-inflammatory tumor microenvironment. One of the chemokines, CCL5, has been linked to disease progression of multiple cancers including prostate cancer (35). Likewise, increased NF-κB signaling predicts prostate cancer progression in prostate (32, 36). Hence, our finding that prostate tumors of current smokers tend to have an immune signature and NF-κB activation is consistent with their increased metastatic potential.

Nicotine has oncogenic properties that meet the criteria of a pro-metastatic factor (10). Because we could not directly examine the effects of nicotine in cancer patients, we investigated them in cell culture and TRAMP mice and observed that nicotine increases glutamine consumption of cancer cells and enhances invasion and metastasis. Increased glutamine consumption is a hallmark of cancer and predicts poor survival in breast cancer (37). In TRAMP mice, primary tumors from nicotine-treated animals showed increased expression of genes regulating synaptic signal transduction, whereas nicotine-driven Akt pathway activation was prominent in cell culture. Akt signaling enhances prostate cancer progression (38, 39). The cancer-promoting effects of nicotine have also been evaluated in animal models of lung cancer. While one study reported that nicotine promotes tumor growth and metastasis (40), two other studies could not find a nicotine effect on tumor growth (41, 42). Thus, the effect of nicotine on tumor growth is controversial and model-dependent. Moreover, metastasis-related rather than tumor growth-related phenotypes may develop in nicotine-treated animals. We believe that the use of TRAMP mice was justified

because this model captures a neuroendocrine differentiation that is also observed in CRPC (43). Nicotine may promote progression of cancers with neuroendocrine features such as a subset of castration-resistant tumors and metastatic prostate cancers, or the aggressive small cell lung cancer (44). In addition, autonomic nerve development has recently been shown to contribute to prostate cancer progression (45). Noteworthy, in this context, is our finding that nicotine increased expression of genes in synaptic signal transduction, thus potentially increasing nerve development and signaling.

Finally, we found that circulating IL-8 levels are increased in current smokers with prostate cancer. IL-8 expression can be induced by nicotine in human neutrophils (46), and its expression correlates with metastasis in prostate cancer (47, 48). While nicotine may induce IL-8 directly, up-regulated IL-8 in smokers may also arise from other mechanisms, e.g., activation of monocytes by various smoking-related xenobiotics. Nonetheless, the finding of increased IL-8 in current smokers with prostate cancer reveals another candidate mechanism by which tobacco use following a prostate cancer diagnosis could enhance metastasis.

In summary, our study uncovered several mechanisms by which smoking may increase metastasis in prostate cancer patients. However, our study has few limitations; for example, we used TRAMP mice to show that nicotine accelerates metastasis *in vivo*. These animals develop mainly neuroendocrine tumors that are different from typical adenocarcinomas. Nevertheless, our findings point to the need of additional mechanistic and population-based studies, to define the relative contribution of nicotine to prostate cancer metastasis in current smokers.

Supplementary Material

Refer to Web version on PubMed Central for supplementary material.

ACKNOWLEDGEMENTS

We thank CPCTR for providing tissue specimens and supporting data. We would also like to thank personnel at the University of Maryland and the Baltimore Veterans Administration Hospital for their contributions with the recruitment of subjects.

Financial support: This research was supported by the Intramural Research Program of the NIH, National Cancer Institute (NCI), Center for Cancer Research, and was also funded with federal funds from the NCI under Contract No. HHSN261200800001E. In addition, grants to Arun Sreekumar and Nagireddy Putluri supported this work (W81XWH-12-1-0130 from DOD, DMS 1161759 from NSF, NIH U01 CA167234, CPRIT Metabolomics Core-RP120092 Alkek CMD Grants).

REFERENCES

1. Jemal A, Bray F, Center MM, Ferlay J, Ward E, Forman D. Global cancer statistics. CA Cancer J.Clin. 2011; 61:69–90. [PubMed: 21296855]
2. Hsing AW, Chokkalingam AP. Prostate cancer epidemiology. Front Biosci. 2006; 11:1388–1413. [PubMed: 16368524]
3. Giovannucci E, Rimm EB, Ascherio A, Colditz GA, Spiegelman D, Stampfer MJ, Willett WC. Smoking and risk of total and fatal prostate cancer in United States health professionals. Cancer Epidemiol.Biomarkers Prev. 1999; 8:277–282. [PubMed: 10207628]
4. Hickey K, Do KA, Green A. Smoking and prostate cancer. Epidemiol.Rev. 2001; 23:115–125. [PubMed: 11588835]

5. Huncharek M, Haddock KS, Reid R, Kupelnick B. Smoking as a risk factor for prostate cancer: a meta-analysis of 24 prospective cohort studies. Am.J.Public Health. 2010; 100:693–701. [PubMed: 19608952]
6. Kenfield SA, Stampfer MJ, Chan JM, Giovannucci E. Smoking and prostate cancer survival and recurrence. JAMA. 2011; 305:2548–2555. [PubMed: 21693743]
7. Roberts WW, Platz EA, Walsh PC. Association of cigarette smoking with extraprostatic prostate cancer in young men. J Urol. 2003; 169:512–516. [PubMed: 12544299]
8. Kobrinsky NL, Klug MG, Hokanson PJ, Sjolander DE, Burd L. Impact of smoking on cancer stage at diagnosis. J.Clin.Oncol. 2003; 21:907–913. [PubMed: 12610192]
9. West KA, Brognard J, Clark AS, Linnoila IR, Yang X, Swain SM, Harris C, Belinsky S, Dennis PA. Rapid Akt activation by nicotine and a tobacco carcinogen modulates the phenotype of normal human airway epithelial cells. J Clin Invest. 2003; 111:81–90. [PubMed: 12511591]
10. Schuller HM. Is cancer triggered by altered signalling of nicotinic acetylcholine receptors? Nat.Rev.Cancer. 2009; 9:195–205. [PubMed: 19194381]
11. Melamed J, Datta MW, Becich MJ, Orenstein JM, Dhir R, Silver S, Fidelia-Lambert M, Kadjacsy-Balla A, Macias V, Patel A, Walden PD, Bosland MC, Berman JJ. The cooperative prostate cancer tissue resource: a specimen and data resource for cancer researchers. Clin Cancer Res. 2004; 10:4614–4621. [PubMed: 15269132]
12. Wallace TA, Prueitt RL, Yi M, Howe TM, Gillespie JW, Yfantis HG, Stephens RM, Caporaso NE, Loffredo CA, Ambs S. Tumor immunobiological differences in prostate cancer between African-American and European-American men. Cancer Res. 2008; 68:927–936. [PubMed: 18245496]
13. Gentleman RC, Carey VJ, Bates DM, Bolstad B, Dettling M, Dudoit S, Ellis B, Gautier L, Ge Y, Gentry J, Hornik K, Hothorn T, Huber W, Iacus S, Irizarry R, Leisch F, Li C, Maechler M, Rossini AJ, Sawitzki G, Smith C, Smyth G, Tierney L, Yang JY, Zhang J. Bioconductor: open software development for computational biology and bioinformatics. Genome Biol. 2004; 5:R80. [PubMed: 15461798]
14. Tusher VG, Tibshirani R, Chu G. Significance analysis of microarrays applied to the ionizing radiation response. Proc.Natl.Acad.Sci.U.S.A. 2001; 98:5116–5121. [PubMed: 11309499]
15. Subramanian A, Tamayo P, Mootha VK, Mukherjee S, Ebert BL, Gillette MA, Paulovich A, Pomeroy SL, Golub TR, Lander ES, Mesirov JP. Gene set enrichment analysis: a knowledge-based approach for interpreting genome-wide expression profiles. Proc Natl Acad Sci U.S.A. 2005; 102:15545–15550. [PubMed: 16199517]
16. Grabus SD, Martin BR, Batman AM, Tyndale RF, Sellers E, Damaj MI. Nicotine physical dependence and tolerance in the mouse following chronic oral administration. Psychopharmacology (Berl). 2005; 178:183–192. [PubMed: 15365686]
17. Kaileh M, Sen R. NF-kappaB function in B lymphocytes. Immunol.Rev. 2012; 246:254–271. [PubMed: 22435560]
18. Van Waes C, Chang AA, Lebowitz PF, Druzgal CH, Chen Z, Elsayed YA, Sunwoo JB, Rudy SF, Morris JC, Mitchell JB, Camphausen K, Gius D, Adams J, Sausville EA, Conley BA. Inhibition of nuclear factor-kappaB and target genes during combined therapy with proteasome inhibitor bortezomib and reirradiation in patients with recurrent head-and-neck squamous cell carcinoma. Int.J Radiat.Oncol.Biol Phys. 2005; 63:1400–1412. [PubMed: 16005577]
19. Russell MA, Jarvis M, Iyer R, Feyerabend C. Relation of nicotine yield of cigarettes to blood nicotine concentrations in smokers. Br.Med.J. 1980; 280:972–976. [PubMed: 7417765]
20. Benowitz NL, Kuyt F, Jacob P III. Circadian blood nicotine concentrations during cigarette smoking. Clin.Pharmacol.Ther. 1982; 32:758–764. [PubMed: 7140139]
21. Rutella S, Bonanno G, Procoli A, Mariotti A, de Ritis DG, Curti A, Danese S, Pessina G, Pandolfi S, Natoni F, Di Febo A, Scambia G, Manfredini R, Salati S, Ferrari S, Pierelli L, Leone G, Lemoli RM. Hepatocyte growth factor favors monocyte differentiation into regulatory interleukin (IL)-10++IL-12low/neg accessory cells with dendritic-cell features. Blood. 2006; 108:218–227. [PubMed: 16527888]
22. Peng T, Golub TR, Sabatini DM. The immunosuppressant rapamycin mimics a starvation-like signal distinct from amino acid and glucose deprivation. Mol Cell Biol. 2002; 22:5575–5584. [PubMed: 12101249]

23. Bobrovnikova-Marjon EV, Marjon PL, Barbash O, Vander Jagt DL, Abcouwer SF. Expression of angiogenic factors vascular endothelial growth factor and interleukin-8/CXCL8 is highly responsive to ambient glutamine availability: role of nuclear factor-kappaB and activating protein-1. Cancer Res. 2004; 64:4858–4869. [PubMed: 15256456]
24. Egleton RD, Brown KC, Dasgupta P. Nicotinic acetylcholine receptors in cancer: multiple roles in proliferation and inhibition of apoptosis. Trends Pharmacol.Sci. 2008; 29:151–158. [PubMed: 18262664]
25. Hall CL, Dai J, van Golen KL, Keller ET, Long MW. Type I collagen receptor (alpha 2 beta 1) signaling promotes the growth of human prostate cancer cells within the bone. Cancer Res. 2006; 66:8648–8654. [PubMed: 16951179]
26. Hall CL, Dubyk CW, Riesenberger TA, Shein D, Keller ET, van Golen KL. Type I collagen receptor (alpha2beta1) signaling promotes prostate cancer invasion through RhoC GTPase. Neoplasia. 2008; 10:797–803. [PubMed: 18670640]
27. Gingrich JR, Barrios RJ, Morton RA, Boyce BF, DeMayo FJ, Finegold MJ, Angelopoulou R, Rosen JM, Greenberg NM. Metastatic prostate cancer in a transgenic mouse. Cancer Res. 1996; 56:4096–4102. [PubMed: 8797572]
28. Moreira DM, Nickel JC, Gerber L, Muller RL, Andriole GL, Castro-Santamaria R, Freedland SJ. Smoking Is Associated with Acute and Chronic Prostatic Inflammation: Results from the REDUCE Study. Cancer Prev.Res.(Phila). 2015; 8:312–317. [PubMed: 25644151]
29. Lee PN, Hamling J. Systematic review of the relation between smokeless tobacco and cancer in Europe and North America. BMC.Med. 2009; 7:36. [PubMed: 19638245]
30. Schuller HM, Tithof PK, Williams M, Plummer H III. The tobacco-specific carcinogen 4-(methylnitrosamino)-1-(3-pyridyl)-1-butanone is a beta-adrenergic agonist and stimulates DNA synthesis in lung adenocarcinoma via beta-adrenergic receptor-mediated release of arachidonic acid. Cancer Res. 1999; 59:4510–4515. [PubMed: 10493497]
31. Woo JR, Liss MA, Muldong MT, Palazzi K, Strasner A, Ammirante M, Varki N, Shabaik A, Howell S, Kane CJ, Karin M, Jamieson CA. Tumor infiltrating B-cells are increased in prostate cancer tissue. J.Transl.Med. 2014; 12:30. [PubMed: 24475900]
32. Ammirante M, Luo JL, Grivennikov S, Nedospasov S, Karin M. B-cell-derived lymphotoxin promotes castration-resistant prostate cancer. Nature. 2010; 464:302–305. [PubMed: 20220849]
33. de Visser KE, Korets LV, Coussens LM. De novo carcinogenesis promoted by chronic inflammation is B lymphocyte dependent. Cancer Cell. 2005; 7:411–423. [PubMed: 15894262]
34. Gunderson AJ, Coussens LM. B cells and their mediators as targets for therapy in solid tumors. Exp.Cell Res. 2013; 319:1644–1649. [PubMed: 23499742]
35. Aldinucci D, Colombatti A. The inflammatory chemokine CCL5 and cancer progression. Mediators.Inflamm. 2014; 2014:292376. [PubMed: 24523569]
36. Jin R, Yi Y, Yull FE, Blackwell TS, Clark PE, Koyama T, Smith JA Jr. Matusik RJ. NF-kappaB gene signature predicts prostate cancer progression. Cancer Res. 2014; 74:2763–2772. [PubMed: 24686169]
37. Terunuma A, Putluri N, Mishra P, Mathe EA, Dorsey TH, Yi M, Wallace TA, Issaq HJ, Zhou M, Killian JK, Stevenson HS, Karoly ED, Chan K, Samanta S, Prieto D, Hsu TY, Kurley SJ, Putluri V, Sonavane R, Edelman DC, Wulff J, Starks AM, Yang Y, Kittles RA, Yfantis HG, Lee DH, Ioffe OB, Schiff R, Stephens RM, Meltzer PS, Veenstra TD, Westbrook TF, Sreekumar A, Ambs S. MYC-driven accumulation of 2-hydroxyglutarate is associated with breast cancer prognosis. J.Clin.Invest. 2014; 124:398–412. [PubMed: 24316975]
38. Dong G, Chen Z, Li ZY, Yeh NT, Bancroft CC, Van Waes C. Hepatocyte growth factor/scatter factor-induced activation of MEK and PI3K signal pathways contributes to expression of proangiogenic cytokines interleukin-8 and vascular endothelial growth factor in head and neck squamous cell carcinoma. Cancer Res. 2001; 61:5911–5918. [PubMed: 11479233]
39. Kreisberg JI, Malik SN, Prihoda TJ, Bedolla RG, Troyer DA, Kreisberg S, Ghosh PM. Phosphorylation of Akt (Ser473) is an excellent predictor of poor clinical outcome in prostate cancer. Cancer Res. 2004; 64:5232–5236. [PubMed: 15289328]

40. Davis R, Rizwani W, Banerjee S, Kovacs M, Haura E, Coppola D, Chellappan S. Nicotine promotes tumor growth and metastasis in mouse models of lung cancer. PLoS.ONE. 2009; 4:e7524. [PubMed: 19841737]

41. Murphy SE, von Weymarn LB, Schutten MM, Kassie F, Modiano JF. Chronic nicotine consumption does not influence 4-(methylnitrosamino)-1-(3-pyridyl)-1-butanone-induced lung tumorigenesis. Cancer Prev.Res (Phila). 2011; 4:1752–1760. [PubMed: 22027684]

42. Maier CR, Hollander MC, Hobbs EA, Dogan I, Linnoila RI, Dennis PA. Nicotine does not enhance tumorigenesis in mutant K-ras-driven mouse models of lung cancer. Cancer Prev.Res (Phila). 2011; 4:1743–1751. [PubMed: 22027685]

43. Yuan TC, Veeramani S, Lin FF, Kondrikou D, Zelivianski S, Igawa T, Karan D, Batra SK, Lin MF. Androgen deprivation induces human prostate epithelial neuroendocrine differentiation of androgen-sensitive LNCaP cells. Endocr.Relat Cancer. 2006; 13:151–167. [PubMed: 16601285]

44. van Meerbeeck JP, Fennell DA, De Ruysscher DK. Small-cell lung cancer. Lancet. 2011; 378:1741–1755. [PubMed: 21565397]

45. Magnon C, Hall SJ, Lin J, Xue X, Gerber L, Freedland SJ, Frenette PS. Autonomic nerve development contributes to prostate cancer progression. Science. 2013; 341:1236361. [PubMed: 23846904]

46. Iho S, Tanaka Y, Takauji R, Kobayashi C, Muramatsu I, Iwasaki H, Nakamura K, Sasaki Y, Nakao K, Takahashi T. Nicotine induces human neutrophils to produce IL-8 through the generation of peroxynitrite and subsequent activation of NF-kappaB. J.Leukoc.Biol. 2003; 74:942–951. [PubMed: 12960242]

47. Kim SJ, Uehara H, Karashima T, Mccarty M, Shih N, Fidler IJ. Expression of interleukin-8 correlates with angiogenesis, tumorigenicity, and metastasis of human prostate cancer cells implanted orthotopically in nude mice. Neoplasia. 2001; 3:33–42. [PubMed: 11326314]

48. Araki S, Omori Y, Lyn D, Singh RK, Meinbach DM, Sandman Y, Lokeshwar VB, Lokeshwar BL. Interleukin-8 is a molecular determinant of androgen independence and progression in prostate cancer. Cancer Res. 2007; 67:6854–6862. [PubMed: 17638896]

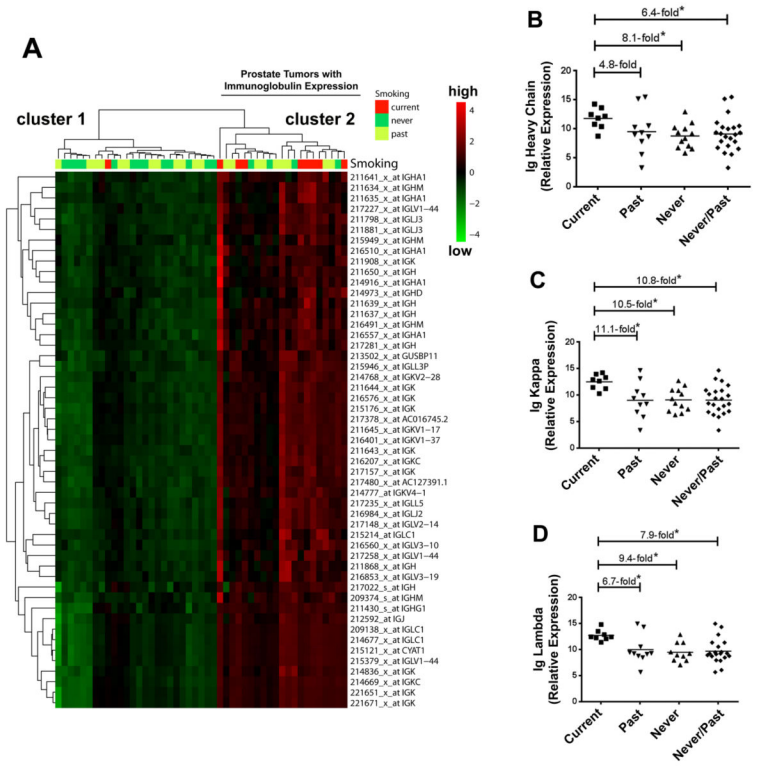

Figure 1. Immunoglobulin expression in prostate tumors from current, past, and never smokers

(**A**) Hierarchical cluster analysis separates 47 prostate tumors (9 current, 21 past, and 17 never smokers) into 2 clusters based on immunoglobulin expression. Heatmap shows up-regulated immunoglobulin expression in cluster 2 (red color intensity). Current smokers are over-represented in this cluster (8/21 vs. 1/26 in cluster 1, $P < 0.01$) while the "low immunoglobulin" cluster 1 was enriched for tumors from never smokers (13/26 vs. 4/21 in cluster 2, $P = 0.03$). Patients' smoking status is shown for each tumor above the heatmap. Shown are array-based expression data with corresponding probeset IDs. (**B-D**) Increased expression of immunoglobulin (Ig) heavy constant mu, kappa constant, and lambda locus in tumors from current smokers by qRT-PCR analysis. *Different at $P < 0.05$ between current smokers (n = 8) and past smokers (n = 10) or never (n = 12). qRT-PCR was performed on a subset of tumors from the microarray analysis.

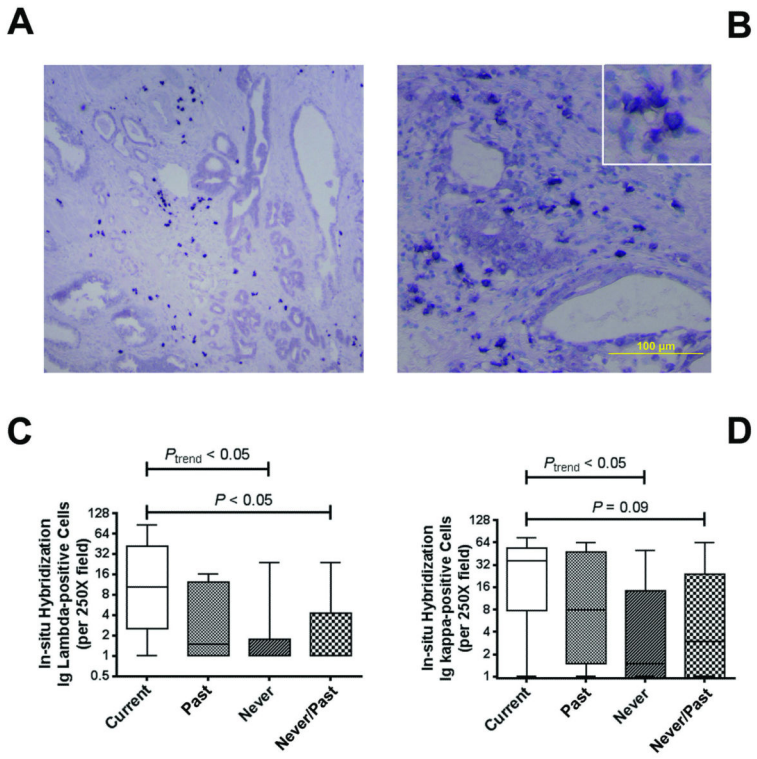

Figure 2. Immunoglobulin expression by *In situ* hybridization

(**A,B**) Shown is the expression of kappa light chain mRNA in a representative prostate tumor from a current smoker in two different fields. *In situ* hybridization (ISH) depicts kappa light chain mRNA expression in lymphocytic infiltrates. The dark blue nitroblue tetrazolium chromogene reveals the predominant stromal localization of the immunoglobulin-positive B lymphocytes. Counterstain: Haematoxylin. (**C,D**) Analysis of ISH results. Numbers of Ig lambda- and Ig kappa-positive B lymphocytes correlated with smoking status [Spearman rank correlation test (P_{trend}) for current (n = 6), past (n = 7), never (n = 9) smokers] and were increased in current smokers versus never/past smokers (Wilcoxon rank-sum test). ISH-positive lymphocytes were counted per 250x field. Shown are box plots with minimum and maximum values (whiskers) and the median as line in the box.

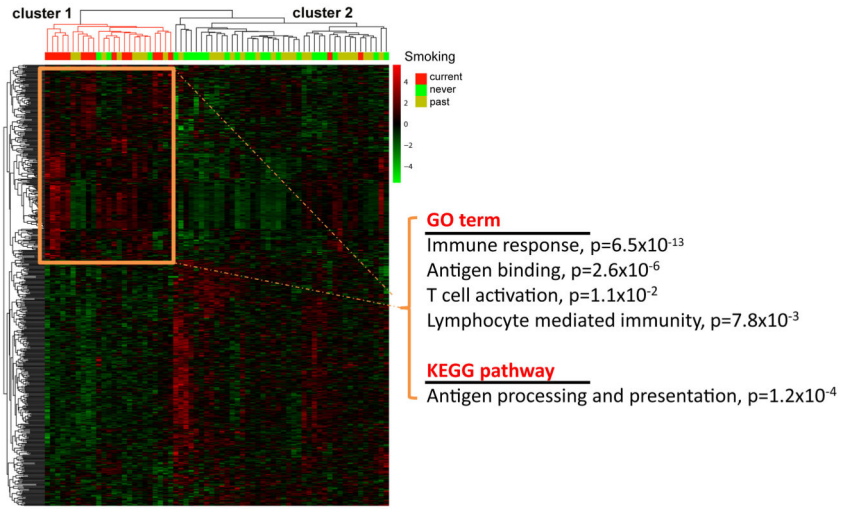

Figure 3. Up-regulation of genes in immune-related pathways is a characteristic of tumors from current smokers

Hierarchical cluster analysis with 601 probesets representing genes that were differentially expressed between current vs. past and current vs.past/never smokers. The expression pattern of these genes separates the 67 tumors (16 current, 28 past, and 23 never smokers) into 2 clusters. Cluster 1 represents tumors with up-regulated expression of immune response-related genes as shown by the Go term and KEGG pathway association. This cluster is highly enriched for tumors from current smokers ($P < 0.001$). Overexpressed genes in cluster 2 did not have a significant pathway or GO term association.

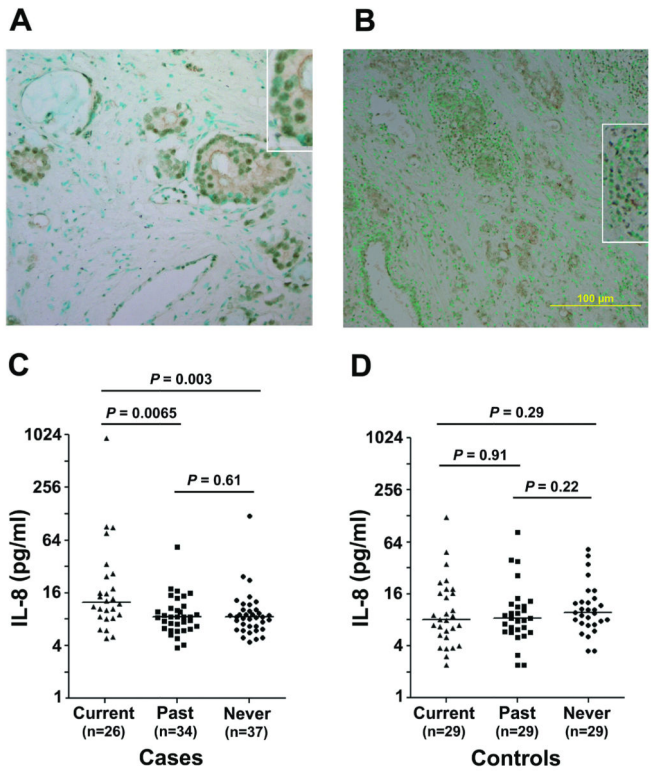

Figure 4. Nuclear accumulation of NF-κB and increased IL-8 among prostate cancer patients who smoke

(**A,B**) Nuclear accumulation of NF-κB P-Ser536 is shown for tumors from a past (**B,** 200x) and current (**D,** 100x) smoker (magnified in the insets). Counterstain: Methyl green. **C.** Cancer patients who are current smokers have increased interleukin-8 (IL-8) plasma levels when compared with past or never smokers. Median increase in current smokers was 1.5-fold. **D.** Current smokers without the disease did not show elevated IL-8 plasma levels. *P* values were calculated with the Mann-Whitney test. A Kruskal-Wallis test for differences between the three smoking groups indicated existing differences among cases ($P = 0.006$) but not the controls ($P = 0.46$).

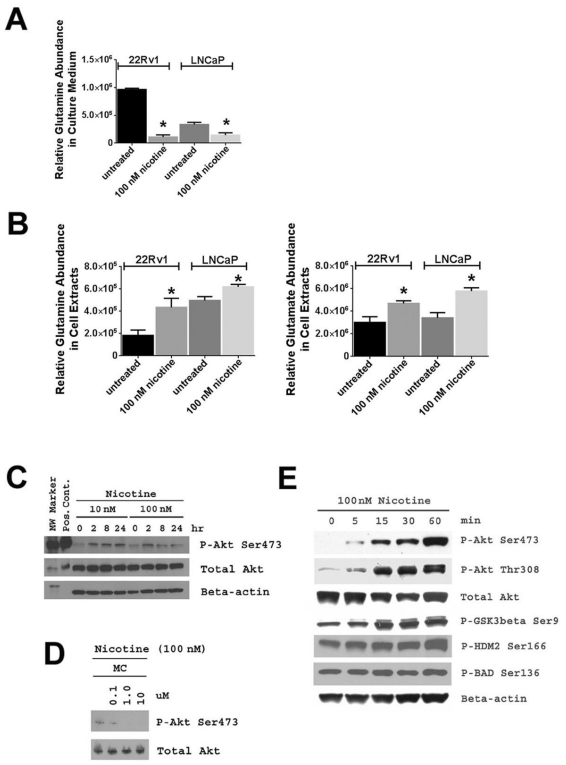

Figure 5. Increased glutamine consumption and Akt activation in nicotine-treated human prostate cancer cells

22Rv1 and LNCaP cells were treated with 100 nM nicotine for 48 hours and glutamine levels were measured in culture medium and cell pellets. **A.** Treatment of 22Rv1 and LNCaP cells with nicotine depleted glutamine in the culture medium. **B.** Nicotine treatment of 22Rv1 and LNCaP cells significantly increased glutamine and glutamate levels in their cell extracts. Glutamate is the intracellular oxidation product of glutamine and was not detectable in cell culture medium. Experiments were done in triplicates. Shown is mean ± SD. * statistically different from untreated (two-sided t-test, $P < 0.05$). **C.** Nicotine at 10 nM and 100 nM concentrations induced Akt phosphorylation in 22Rv1 cells, which was inhibited by mecamylamine (MC), an antagonist of nicotinic acetylcholine receptors (**D**). **E.** Nicotine treatment also induced phosphorylation of known downstream targets of Akt signaling, such as GSK3β, human Mdm2 (HDM2), and BAD. In **D**, cells were exposed to nicotine −/+ MC for 2 hours.

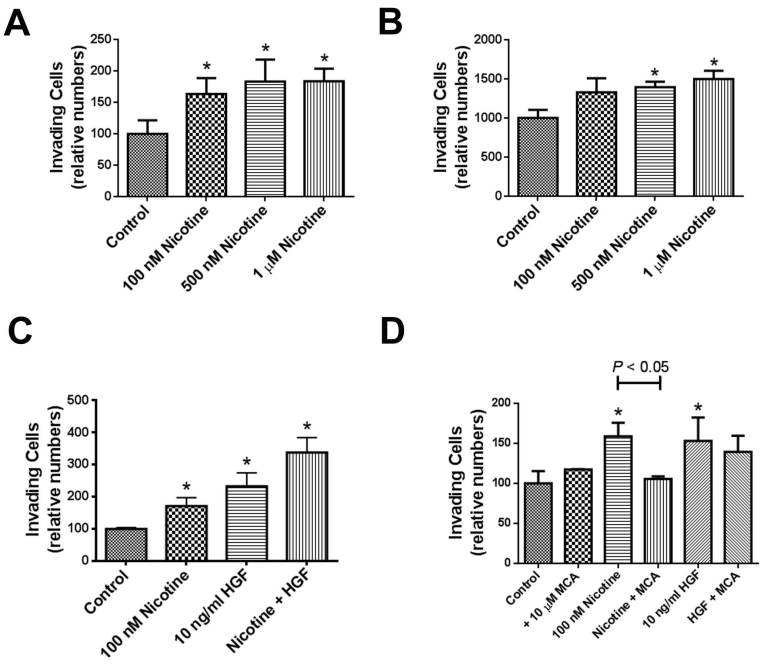

Figure 6. Nicotine enhances matrigel invasion of human prostate cancer cell lines

(**A**) 22Rv1 and (**B**) PC-3 cells were were plated in invasion chambers and were treated with nicotine. (**C**) 22Rv1 cells were treated with nicotine, hepatocyte growth factor (HGF), or both, to assess whether nicotine and HGF have a synergistic effect on matrigel invasion. (**D**) Nicotinic acetylcholine receptor antagonist, mecamylamine (MCA), significantly decreased nicotine-induced increase in matrigel invasion, but not HGF-induced increase in invasion, in 22Rv1 cells. Shown are mean ± SD for n = 3. *Significantly different from control ($P < 0.05$).

Table 1

Lung metastasis in nicotine-treated TRAMP mice

Treatment	**Tap water**	**Nicotine 100 μg/ml**	**Nicotine 250 μg/ml**
# of animals	20	22	23
Lung (number examined)	20	22	23
Lung metastasis	**- (0%)**	**6 * (28%)**	**7 * (31%)**
Adenocarcinoma with metastasis to the lung	- (0%)	1 (5%)	2 (9%)
Neuroendocrine carcinoma with metastasis to the lung	- (0%)	5 (23%)	5 (22%)
Lymph node (# examined)	3	7	3
Lymph node metastasis	- (0%)	2** (29%)	1** (33%)
Urogenital tract weight (mg) without seminal vesicles***			
	592 ± 231	513 ± 195	532 ± 462

* *P* = 0.046; Fisher's exact test for trend;

** neuroendocrine histology;

*** not significantly different between groups in both the animal weight-adjusted and unadjusted analysis ((ANOVA test).